Transverse mode dynamics of VCSELs undergoing current modulation

Peter M. Goorjian*[a], C. Z. Ning[b], Govind P. Agrawal[c]
[a]NASA Ames Research Center, M.S. T27A-2, Moffett Field, CA 94035-1000
[b]NASA Ames Research Center, M.S. N229-1, Moffett Field, CA 94035-1000
[c]The Institute of Optics, University of Rochester, Rochester, NY 14627

ABSTRACT

Transverse mode dynamics of a 20-μm-diameter vertical-cavity surface-emitting laser (VCSEL) undergoing gain switching by deep current modulation is studied numerically. The direct current (dc) level is set slightly below threshold and is modulated by a large alternating current (ac). The resulting optical pulse train and transverse-mode patterns are obtained numerically. The ac frequency is varied from 2.5 GHz to 10 GHz, and the ac amplitude is varied from one-half to four times that of the dc level. At high modulation frequencies, a regular pulse train is not generated unless the ac amplitude is large enough. At all modulation frequencies, the transverse spatial profile switches from single-mode to multiple-mode pattern as the ac pumping level is increased. Optical pulse widths vary in the range 5–30 ps. with the pulse width decreasing when either the frequency is increased or the ac amplitude is decreased. The numerical modeling uses an approximation form of the semiconductor Maxwell–Bloch equations. Temporal evolution of the spatial profiles of the laser (and of carrier density) is determined without any assumptions about the type or number of modes.

Keywords: VCSELs, current modulation, gain switching, transverse mode dynamics, computational modeling

1. INTRODUCTION

Vertical-cavity surface-emitting lasers (VCSELs) have become increasingly important for applications in optical communications and interconnects. For such applications, their high-speed modulation characteristics are important, and so the dynamic characteristics of VCSELs have been extensively studied[1,2] and data transmission at bit rates as high as 10 Gb/s has been demonstrated.[2] One important application of high-speed modulation is the generation of a train of short optical pulses through gain-switching.[3,4] Pulse widths below 20 ps have been generated by this technique.[5] Spatial effects are expected to play an important role in the operation of VCSELs, especially since large-aperture VCSELs often operate in several transverse modes at high injection currents.[6,7] An accurate simulation of gain-switched operation should take into account the temporal evolution of the multiple transverse modes without unduly limiting the number of modes. Previous numerical work studied relatively small diameter VCSELs,[8] in which simulations assumed a small number of transverse modes. In this paper, temporal evolution of the spatial profiles of the laser field and of carrier density is determined for a relatively large diameter VCSEL without any assumptions about the type or number of modes.

Transverse mode dynamics of VCSELs are modeled by an approximation to the semiconductor Maxwell–Bloch equations.[9,10] The time evolution of the spatial profiles of the laser and carrier density is obtained by solving the coupled partial differential equations that govern their evolution by a finite-difference algorithm. The algorithm is fairly general; it can handle devices of any shape, which are either gain or index guided or both. The physical modeling includes the effects of nonlinear carrier dependence and dispersion with respect to wavelength on the optical gain and refractive index. The modeling[9,11,12] of the optical susceptibility is based on first-principles and includes device details such as a quantum well structure and many-body effects. Temporal dynamics as fast as on a picosecond scale can be resolved. This bottom-up approach uses measured material parameters and quantum well structure

* email: goorjian@nas.nasa.gov, cning@nas.nasa.gov, gpa@optics.rochester.edu

parameters, with the number of free parameters minimized. In this paper, the VCSELs are based on InGaAs/GaAs quantum well structures.

Earlier simulations[11,12,14-17] studied transverse mode dynamics of VCSELs under either steady currents or small current modulation away from threshold. These simulations included VCSELs under different pumping levels, and which had different active region shapes and sizes with and without index guiding. The results showed interesting spatio-temporal dynamics. The light fields were time dependent with characteristic time scales on the picosecond time scale. Different types of transverse mode dynamics occurred that included multiple mode beatings, rotating waves, convective waves, and nonlinear locking of transverse modes. Such dynamical behaviors will influence the modulation bandwidth and the beam quality under current modulation. In this paper, a 20-μm-diameter VCSEL undergoing deep current modulation is studied. In Section 2 we provide the equations governing VCSEL dynamics under current modulation and present the computed results in Section 3. Plots of the optical pulse trains are shown first at the ac pumping amplitudes J_{ac}/J_{dc} = 0.5, 1, 2 and 4 for modulation frequencies of ν = 2.5, 5, 7.5 and 10. The corresponding transverse mode patterns are used to interpret the numerical results.

2. GOVERNING EQUATIONS

Assuming a fixed mode profile along the longitudinal direction in VCSELs,[13] the effective Maxwell–Bloch Equations can be written as:[9]

$$\frac{n_g}{c}\frac{\partial E}{\partial t} = \frac{i}{2K}\nabla_\perp^2 E - \kappa E + \frac{iK\Gamma}{2\epsilon_0\epsilon_b}P + \frac{i\delta n(x,y)}{n_b}KE \tag{1}$$

$$\frac{\partial N}{\partial t} = D_N \nabla_\perp^2 N - \gamma_n N + \frac{\eta J(x,y,t)}{e} + \frac{L\Gamma}{2}\frac{i}{4\hbar}(P^*E - PE^*) \tag{2}$$

$$P = P_0 + P_1 \tag{3}$$

$$P_0 = \epsilon_0\epsilon_b\chi_0(N)E \tag{4}$$

$$\frac{dP_1}{dt} = -\Gamma_1(N)P_1 + i(\omega_c - \omega_1(N))P_1 - i\epsilon_0\epsilon_b A_1(N)E \tag{5}$$

$$J(x,y,t) = J_{dc}(x,y) + J_{ac}(x,y)\max(0,\sin(2\pi\nu t)) \tag{6}$$

where $\max(a,b)$ is the larger of a and b.

Here E is the complex laser field envelope amplitude, N is the total carrier density, P_0 and P_1 are the effective material polarization functions that have been constructed from microscopic theory,[9] and $J(x,y,t)$ is the modulated pumping current density. Further, $\delta n(x.y)$ is the guiding index profile arising from, e.g., oxide confinement, $\nabla_\perp^2$ is the Laplacian in the transverse plane, c is the speed of light, ϵ_0 is the permittivity of free space, ω_c is the optical carrier wave frequency in radians per seconds, n_b is the background index of refraction, n_g is the group index of refraction, $\epsilon_b = n_b^2$ is the background relative permittivity, K = $\omega_c n_b/c$ is the optical wavenumber in the cavity with a background index of refraction n_b, κ is the cavity loss, D_N is the carrier diffusion coefficient, γ_n is the nonradiative decay constant or carrier loss rate due to spontaneous and nonradiative processes, η is the quantum efficiency, e is the electron charge, $\hbar = h/2\pi$, where h is Planck's constant, Γ is the confinement factor, and L is the cavity length.

Many-body effects are contained in the density-dependent coefficients $\chi_0(N)$, the effective background susceptibility, $\Gamma_1(N)$, the gain bandwidth, $\omega_1(N)$, the detuning, and $A_1(N)$, the strength of the Lorentzian oscillator. The theoretical basis for the effective Maxwell–Bloch Equations is given in Reference 9. Also, the derivation of the five density-dependent coefficients, which model the optical susceptibility $\chi(\omega,N)$, is given in References 9, 11, 12 and 16.

3. COMPUTED RESULTS

For these calculations, we simulated a VCSEL operating at 980 nm with a circular current aperture of 20 μm in diameter and a cavity length L of 144 nm. The carrier diffusion coefficient was 20 cm^2/s and the confinement factor $\Gamma = 0.25$. The three parameters most important in determining the dynamics are the three decay rates Γ_1, κ, and γ_n. The inverse values of these parameters set the relevant time scales. In our calculations, bandwidth, $1/\Gamma_1(N)$ was approximately 15 fs, (the material polarization P_1 changed on that time scale). Introducing the scaled cavity loss as $\tilde{\kappa} = \kappa/(n_g/c)$, the photon lifetime, $1/\tilde{\kappa}$, was about 2 ps. Finally, the carrier lifetime, $1/\gamma_n$ was 2 ns. At that time scale, the laser field was approximately steady for constant currents.

The dc level for the circular aperture was set at 95% of the threshold value (about 0.7 mA). Calculations were performed for four values of the modulation frequency, viz. ν = 2.5, 5, 7.5 and 10 GHz, and for each frequency, four values of the ac amplitudes were used with J_{ac}/J_{dc} = 0.5, 1, 2 and 4, respectively.

3.1. Gain-Switched Optical Pulse trains

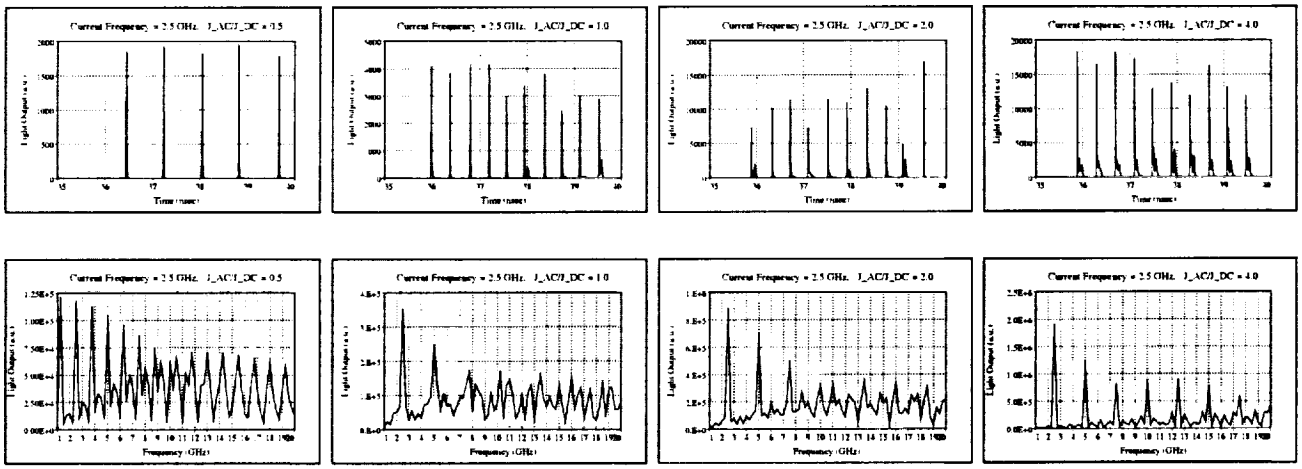

Fig. 1. The light output over 4 ns for current pulses at 2.5 GHz. The first row shows pulse trains at J_{ac}/J_{dc} = 0.5, 1, 2 and 4 respectively. The second row shows the corresponding spectral content for each case.

In this section, we show the results at four modulation frequencies with ν = 2.5, 5, 7.5 and 10 GHz. In each case, the ac amplitude was chosen such that the ratio J_{ac}/J_{dc} had four different values of 0.5, 1, 2 and 4. Figure 1 shows the pulse trains and corresponding spectra for ν = 2.5 GHz. The most noteworthy feature is that the peak heights are not the same even at such a relatively low modulation frequency of 2.5 GHz. At J_{ac}/J_{dc} = 0.5, peak heights are relatively uniform but, at higher values of the ac pumping amplitude, pulse heights vary almost randomly within each train. Note also that pulse spacing is double in the case of J_{ac}/J_{dc} = 0.5. Indeed, the spectrum in this case shows a subharmonic at 1.25 GHz. Its presence indicates that optical pulses are produced every second cycle of the ac modulation when J_{ac}/J_{dc} = 0.5.

For a qualitative understanding of this behavior, we consider the relaxation-oscillation frequency ν_R. Even though the concept of a relaxation-oscillation frequency is, strictly speaking, valid only for small-signal modulation, it can provide some guidelines in the case of large-signal modulation as well. The relaxation-oscillation frequency is given approximately by the formula[18]

$$2\pi\nu_R = \left[(1+f)\gamma_n\tilde{\kappa}\left(\frac{J}{J_{th}} - 1\right)\right]^{\frac{1}{2}} \tag{7}$$

where $J = J_{dc} + J_{ac}$, $J_{dc} = 0.95\ J_{th}$, and f is a constant factor that is approximately equal to 1 for edge-emitting lasers. Chossing $f = 1$ for VCSELs as well, the relaxation-oscillation frequency, ν_R, is approximately equal to 2.4, 3.4, 5 and 7 GHz for $J_{ac}/J_{dc} = 0.5$, 1, 2 and 4, respectively. For $J_{ac}/J_{dc} = 0.5$, ν_R is less than the modulation frequency $\nu = 2.5$ GHz even at peak of the current cycle. If we use the average value of the current, ν_R is so small compared with ν that the VCSEL is not expected to respond at 2.5 GHz. As a result, it is not surprising that the optical pulse builds up after every two cycles, resulting in an effective modulation frequency of 1.25 GHz. For larger ac levels, the relaxation-oscillation frequency becomes comparable to or larger than the modulation frequency, and the VCSEL can generate an optical pulse during each current cycle.

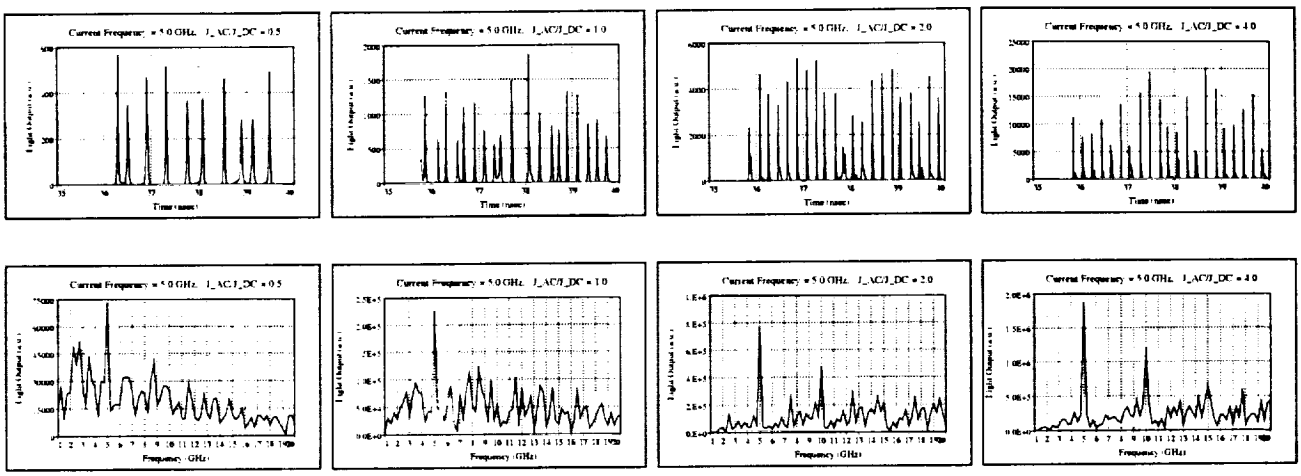

Fig. 2. Same as figure 1 but at a higher a modulation frequency of 5 GHz.

Figure 2–4 show the gain-switched pulse trains and corresponding spectra at higher modulation frequencies of 5, 7.5, and 10 GHz. Now, the relaxation-oscillation frequency becomes less than the current modulation frequency for both $J_{ac}/J_{dc} = 0.5$ and 1.0. Notice in Figure 2 that there are pulses missing occasionally in both cases since the VCSEL cannot respond at 5 GHz until the ac amplitude is increased to $J_{ac}/J_{dc} = 2$ and beyond. Similar behavior is observed in Figs. 3 and 4 for modulation frequencies of 7.5 and 10 GHz. Al low ac amplitudes, the VCSEL does not respond to fast modulations frequencies, and no pulse train is formed. A pulse is produced during each modulation cycle when $J_{ac}/J_{dc} = 4$ since the relaxation-oscillation frequency becomes comparable to the modulation frequency at this pumping level.

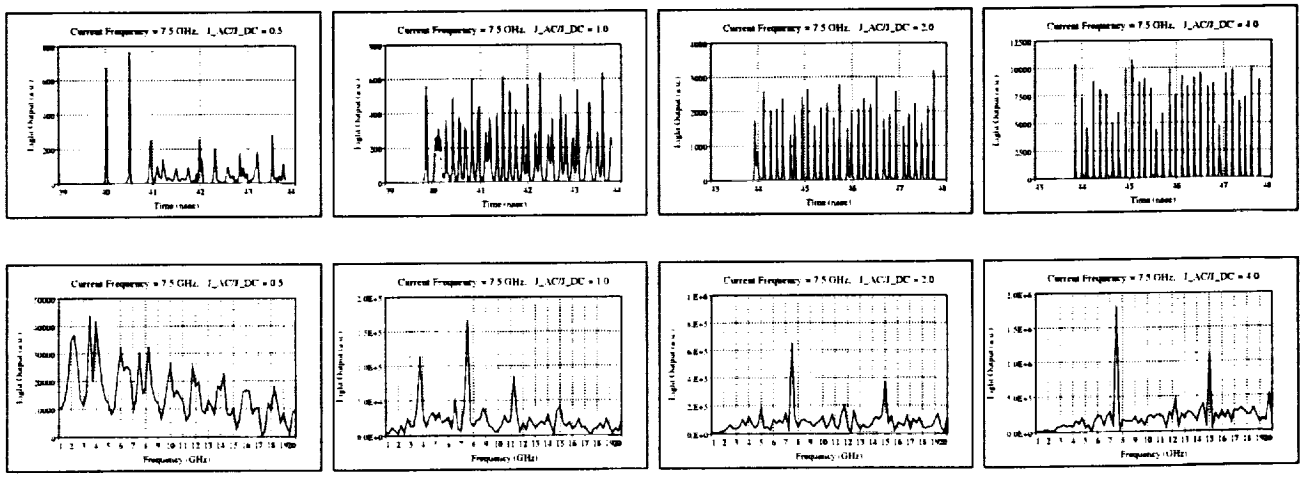

Fig. 3. Same as figure 1 but at a higher modulation frequency of 7.5 GHz.

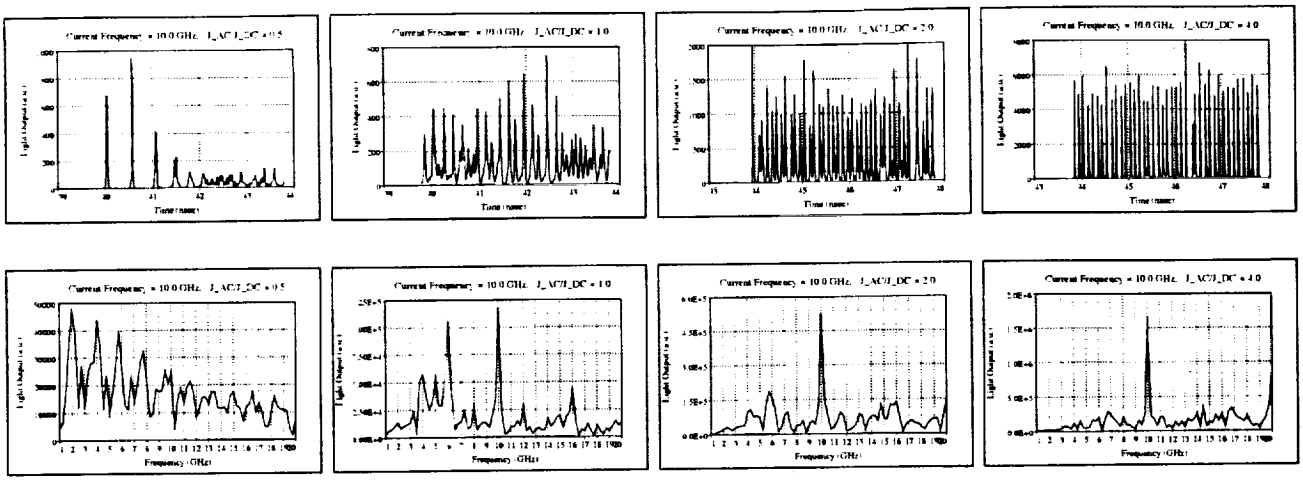

Fig. 4. Same as figure 1 but at still higher modulation frequency of 10 GHz.

We have also investigated how the pulse width changes with the modulation frequency and amplitude. In spite of different pulse heights seen in Figs. 1–4. pulse width is nearly constant for all pulses in a pulse train if the modulation amplitude is large enough for a regular pulse train to form. The average full width at half-maximum (FWHM) in each pulse train is given in Table 1 for all cases for which there were well-defined pulse widths.

	J_{ac}/J_{dc}			
GHZ	0.5	1.0	2.0	4.0
2.5	15ps	12ps	7ps	5ps
5.0	30ps	20ps	10ps	8ps
7.5	N.A.	30ps	15ps	10ps
10.0	N.A.	N.A.	20ps	12ps

3.2. Transverse mode dynamics

An interesting question that one may ask is: what happens to the spatial distribution of the light emitted by VCSEL? More precisely, does the spatial pattern remain the same from pulse to pulse or exhibits dynamic changes on a picosecond time scale? We focus on the lowest modulation frequency of 2.5 GHz. Transverse mode patterns averaged over a full pulse are shown in Figs. 5–8 for four successive pulses at the pumping amplitudes $J_{ac}/J_{dc} = 0.5$, 1, 2 and 4 respectively. The same type of multiple-mode behavior was found to occur at other modulation frequencies studied. In each case, the laser emits a Gaussian-like beam, indicative of single-mode operation, at $J_{ac}/J_{dc} = 0.5$. As the ac amplitude is increased, the VCSEL exhibits a transition from single-mode to multiple transverse modes as seen in Figs. 5–8. The pattern becomes more complex as J_{ac}/J_{dc} becomes large since more and more transverse modes get excited. In the last three cases, the spatial pattern also changes from pulse to pulse, indicating the non-stationary nature of the spatial profile.

What is the relationship between the oscillating spatial pattern and the gain-switched pulse trains? The two are coupled through the gain-saturation and spatial hole-burning effects. Consider first the case $J_{ac}/J_{dc} = 0.5$. Since a single transverse mode is excited in this near-threshold case, a spatial hole is burned in the center where the intensity is largest. Since it takes some time, before the hole can be filled by carrier diffusion (about 1 ns) and since the modulation period is shorter than this time in all cases, it is evident that the hole will never be completely filled. As a result, the gain available during each cycle will vary from pulse to pulse. This is the main reason why different pulses in pulse trains shown in Fig. 1 have different heights. At higher pumping levels, the spatial pattern becomes much more complex because of the onset of higher-order modes. Moreover, different modes are excited during successive modulation cycles. One can understand this behavior using the concept of spatial hole-burning. During a specific

gain-switched pulse, spatial holes occur in the carrier density at locations where the spatial pattern is more intense. During the next modulation cycle, these holes cannot be filled completely by carrier diffusion because of the lack of sufficient time. As a result, a different set of transverse modes participates in the formation of the gain-switched pulse. This pulse burns its own set of spatial holes at different locations. The process repeats and is responsible for unequal pulse heights and different spatial patterns occurring for different modulation cycles.

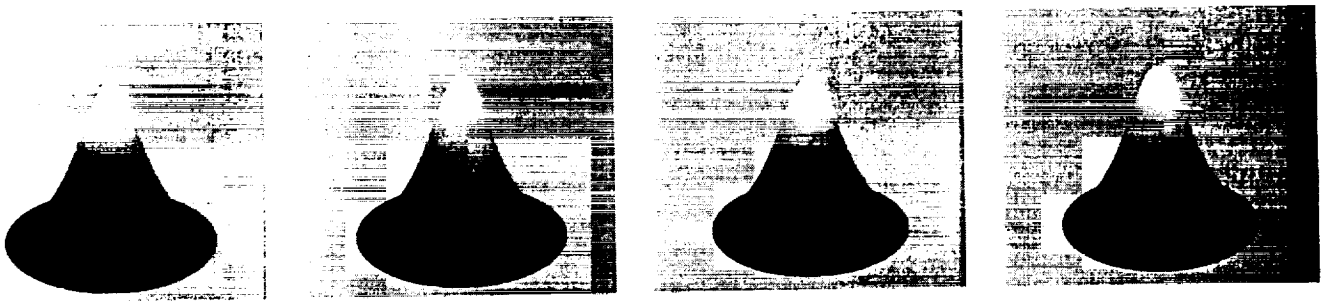

Fig. 5. The transverse mode patterns of the light fields from four of the pulses from a current modulation at 2.5 GHZ with $J_{ac}/J_{dc} = 0.5$

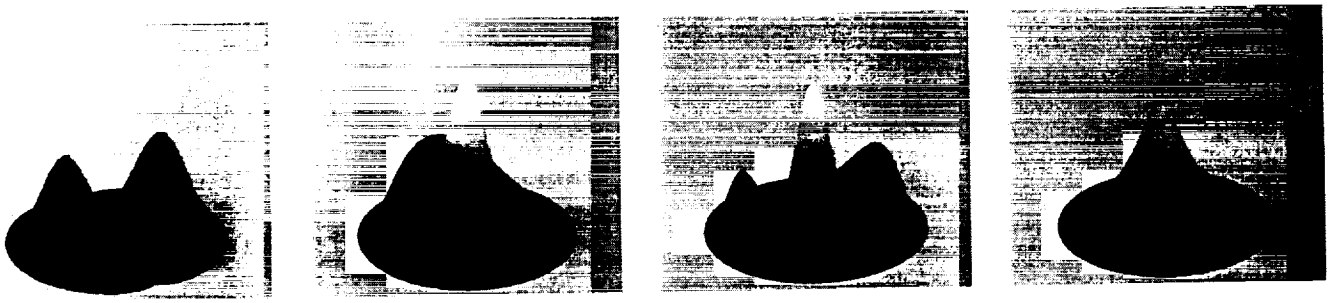

Fig. 6. Same as figure 5 but for $J_{ac}/J_{dc} = 1.0$

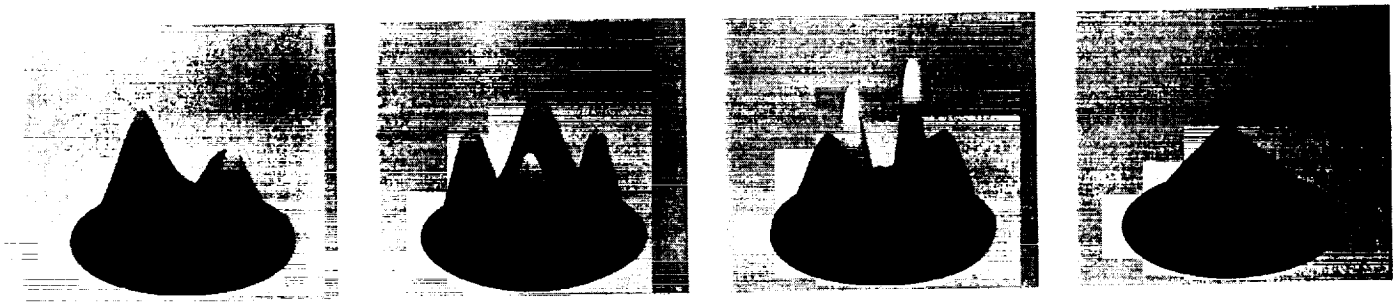

Fig. 7. Same as figure 5 but for $J_{ac}/J_{dc} = 2.0$

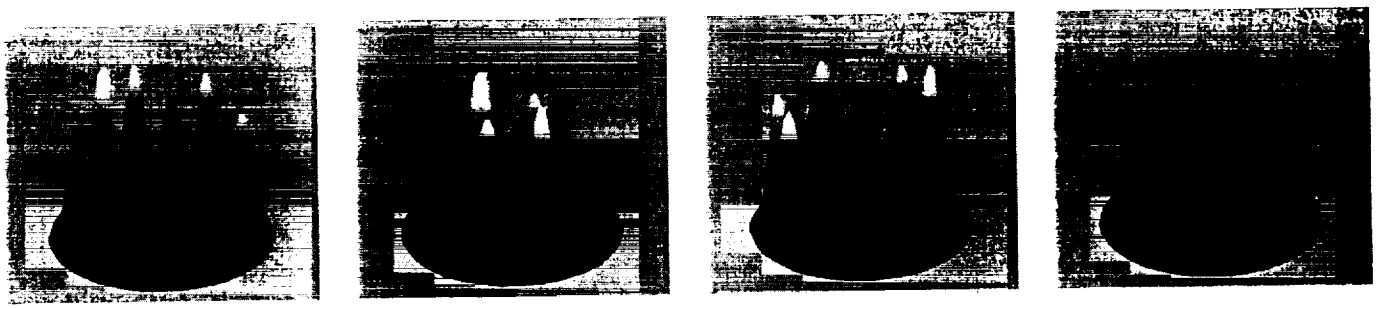

Fig. 8. Same as figure 5 but for $J_{ac}/J_{dc} = 4.0$

4. CONCLUSION

The performance of a 20-μ-diameter VCSEL, modulated deeply to produce a gain-switched pulse train, was studied numerically. It was found that a well-defined pulse train is formed only if the amplitude of the ac pumping level is large enough that the relaxation-oscillation frequency value of the current is comparable to the modulation frequency. Even when this condition is satisfied, pulse heights in the gain-switched train are not the same and appear to have random amplitudes. These results indicate that large-signal modulation and gain switching of VCSELs at high repetition rates may not be practical in large-area VCSELs.

A novel feature of our numerical model is its ability to predict the spatial distribution of the emitted light even for heavily multimoded VCSELs. Our results indicate that the transverse spatial patterns are quite complex in gain-switched VCSELs and change from pulse to pulse. This behavior is attributed to the gain saturation and spatial hole-burning effects.

REFERENCES

1. S. F. YU, "Dynamic behavior of vertical-cavity surface-emitting lasers," *IEEE J. Quanum Electron.*, vol. 32, No. 7, pp. 1168-1179. 1996.
2. U. Fielder, G. Reiner, P. Schnitzer, and K. J. Ebeling, "Top surface-emitting vertical-cavity laser diodes for 10-Gb/s data transmission," *IEEE Photon. Technol. Lett.*, vol. 8, pp. 746-748, 1996.
3. O. Buccafusca, J. L. A. Chilla, J. J. Rocca, S. Field, C. Wilmsen, V. Morozov, and R. Leibenguth, "Transverse mode dynamics in vertical cavity surface emitting lasers excited by fast electrical pulses," *Apppl. Phys. Lett.*, vol.68, No. 5, pp. 590-592, 1996.
4. J. M. Weisenfeld, G. Hasnain, J. S. Perino, J. D. Wynn, R. E. Leibenguth, Y. Wang and A. Y. Cho," Gain-switched GaAs vertical cavity surface emitting lasers," *IEEE J. Quanum Electron.*, vol. 29, No. 6, pp. 1996-2005, June 1993.
5. P. Pepelijugoski, J. Lin, J. Gamelin, M. Hong, and K. Y. Lau, "Ultralow timing jitter in electrically gain-switched vertical cavity surface emitting lasers," *Apppl. Phys. Lett.*, vol.62, pp. 1588-1590, 1993.
6. C. J. Chang-Hasnain, J. P. Harbison, G. Hasnain, A. C. Von Lehmen, L. T. Florez, and N. G. Stoffel, "Dynamic, polarization and transverse mode characteristics of VCSELs, *IEEE J. Quanum Electron.*, vol. 27, No. 6, pp. 1402-1408, 1991.
7. A. Valle, J. Sarma, and K. Shore, "Dynamics of transverse mode competition in VCSEL diodes," *Opt. Commun.*, vol.115, pp. 297-302, 1995.
8. J. Y. Law and Govind P. Agrawal, "Effects of spatial hole burning on gain switching in vertical cavity surface emitting lasers," *IEEE J. Quanum Electron.*, vol. 33, No.3, pp. 462-468, 1997.
9. C. Z. Ning, R. A. Indik and J. V. Moloney, "Effective Bloch-equations for semiconductor lasers and amplifiers," *IEEE J. Quan. Electron.*, vol. 33. pp. 1543-1550, (1997).

10. T. Rossler, R. A. Indik, G. K. Harkness, J. V. Moloney, C. Z. Ning, "Modeling the interplay of thermal effects and transverse mode behavior in native-oxide-confined vertical-cavity surface-emitting lasers," *Phys. Rev. A*, vol. 58, pp. 3279-3292, (1998)
11. P. M. Goorjian and C. Z. Ning, "Transverse mode dynamics of VCSELs through space-time simulation," *Optics Express*, vol. 5, No.3, pp. 55-62, 1999.
12. C. Z. Ning and P. M. Goorjian, "Microscope modeling and simulation of transverse mode dynamics of vertical-cavity surface-emitting lasers," special issue on "spacial and polarization dynamics of semiconductor lasers," edited by G. P. Agrawal, C. Z. Ning and M. San Mignel, *J. Opt. Soc. Am. B*, vol. 16, pp. 2072-2082, (1999).
13. C. Z. Ning, R. A. Indik, and J. V. Moloney, "A self-consistent approach to thermal effects in vertical-cavity surface-emitting lasers," *J. Opt. Soc. Am. B*, vol. 12, pp. 1993-2004, 1995.
14. P. M. Goorjian, and C. Z. Ning, "Computational modeling of vertical-cavity surface-emitting lasers," paper Thc15, nonlinear optics topical meeting, Kauai, HI, August 9-14, 1998.
15. P. M. Goorjian, and C. Z. Ning, "Simulation of transverse modes in vertical-cavity surface-emitting lasers," 1998 annual meeting of the Optical Society of America, Baltimore, MD, October 5-9, 1998.
16. P. M. Goorjian, and C. Z. Ning, "Transverse mode dynamics of VCSELs through space-time simulation," "physics and simulation of optoelectronic devices VII," SPIE-Proceedings, Vol.3625, pp. 375-401, (1999).
17. P. M. Goorjian and C. Z. Ning, "Transverse mode dynamics of VCSELs under current modulation," paper RMG3, integrated photonics research topical meeting, (IPR'99), July 19-23, 1999, Santa Barbara, CA., cosponsored by Optical Society of America and IEEE/Lasers and Electro-Optics Society.
18. G. P. Agrawal and N. K. Dutta, *Semiconductor Lasers*, 2nd Ed., Van Norstrand Reinhold, New York, 1993.